

AN ADAPTIVE FINITE ELEMENT METHOD FOR SHAPE OPTIMIZATION IN STATIONARY INCOMPRESSIBLE FLOW WITH DAMPING

JIAN SU, ZHANGXIN CHEN, ZHIHENG WANG, AND GUANG XI

Abstract. This paper develops an adaptive finite element method for shape optimization in stationary incompressible flow with damping. The continuous shape gradient of an objective functional with respect to the boundary shape is derived by using the adjoint equation method and a function space parametrization technique. A projection a-posteriori error estimator is proposed, which can be computed easily and implemented in parallel. Based on this error estimator, an adaptive finite element method is constructed to solve state and adjoint equations and a regularized equation in each iteration step. Finally, the effectiveness of this adaptive method is demonstrated by numerical experiments.

Key words. Shape gradient, a-posteriori error estimator, projection operator, adaptive finite element method, numerical experiments.

1. Introduction

A shape optimization problem is to find a domain in a set of admissible domains such that an objective functional achieves a minimum or maximum on it [22]. The research of shape optimization is a branch of optimal control governed by partial differential equations [15] and has a very wide range of applications in engineering such as in the design of aircraft wings, high-speed train heads, impeller blades, and bridges in medically bypassing surgeries. In the last few decades, the shape optimization problems have attracted the interest of many applied mathematicians and engineers [11-14, 16-18, 22, 23, 26, 27].

Numerical methods for shape optimization problems can be classified into gradient-based and non-gradient-based optimization methods. The non-gradient-based methods include the one-shot method [11], approximate model methods [13, 18], and evolutionary methods [16, 17]. The one-shot method does not involve an optimization iteration and only needs to solve an optimality system which consists of coupled state and adjoint equations and an optimality condition. The one-shot method seems very attractive but it is not feasible to solve a coupled large-scale nonlinear system in many flow optimization and control problems [11]. The approximate model methods such as the response surface method and the Kriging method depend on the choice of a sample space. If the early samples cannot reflect the characteristics of the design space, these methods will fail to find an optimal shape. The evolutionary methods may be able to find a global minimum or maximum when the strained state equations are easy to solve. However, these methods are difficult to use in reality when a cost function in them is difficult to calculate, because they involve hundreds or even thousands of calculations to locate a near-optimal solution even for fairly simple cases.

Received by the editors January 2, 2014 and, in revised form, March 5, 2014.

2000 *Mathematics Subject Classification.* 65N30, 49J20.

This research was supported by the National Natural Science Foundation of China (No. 11001216, 11171269, 51236006, 11371288), China Scholarship Council (No. 201206285018) and China Postdoctoral Science Foundation(No.2012M521771).

Relatively, the gradient-based methods have the advantage of fast convergence and high efficiency. For these methods, the most crucial step is how to compute the gradient of an objective functional with respect to a shape variable. The approaches to obtain the shape gradient include the finite difference [11], sensitivity [12, 22] and adjoint equation approaches [14, 26, 27, 30]. The finite difference approach finds a gradient by using a difference quotient approximation. Thus, if N design variables are used to describe a domain shape, then one needs to solve the constrained state equations $N + 1$ times at each iteration step of the optimization algorithm. This approach can be extremely expensive in practical applications involving a large number of design variables. The sensitivity approach utilizes a sensitivity equation to obtain the shape gradient by the chain rule, and only requires to solve the state equations one time and linear sensitivity systems N times at each optimization cycle. In contrast, to compute all components of the gradient of the functional using the adjoint equation approach requires the solutions of a single linear adjoint equation and state equations one time. This approach produces a gradient of the objective functional without a cost increase with an increasing number of shape design parameters.

In every optimal cycle, how to increase the accuracy of numerical approximations for a shape gradient is still a big challenge. The overall accuracy of the numerical approximations often deteriorates due to local singularities such as those arising from corners of domains and interior or boundary layers. An obvious strategy is to refine the grids near these critical regions, i.e., to insert more grid points where the singularities occur. A mathematical theory is developed for an adaptive finite element method based on a class of a-posteriori error estimators by Babuška and Rheinboldt [1]. Yan and Liu et al derived a-posteriori error estimates for a finite element approximation of distributed optimal control problems governed by the Stokes equations [2] and parabolic equations [31]. Bangerth introduced a framework for the adaptive finite element solution of a coefficient estimation problem in partial differential equations [3]. In 2010, Zee et al. developed duality-based a-posteriori error estimates and adaptivity for free boundary problems via shape-linearization principles [4].

In this paper, we study an adaptive finite element method for shape optimization in stationary incompressible flow with damping. First, we use a velocity method to describe a variational domain in the optimization process. Second, the adjoint equations are derived by employing the differentiability of an saddle point problem which includes a Lagrange multiplier function. We obtain the continuous gradient of an objective functional with respect to the domain shape with these adjoint equations and a function space parametrization technique. Third, motivated by the stabilized finite element method based on the two local Gauss integrals technique in recent years [19-21, 24, 25], we construct an a-posteriori error estimator by a projection operator. Fourth, we present the adaptive finite element method for the state and adjoint equations and a regularized gradient equation based on this error estimator. Finally, the effectiveness of this adaptive method is demonstrated by numerical experiments.

This paper is organized as follows: In Section 2, we state the shape optimization problem in stationary incompressible flow with damping and derive the continuous shape gradient. In Section 3 we propose an adaptive finite element method based on a projection a-posteriori error estimator. We then present numerical examples in Section 4, followed by conclusions in Section 5.

Similar to the method in [10], we have the existence and uniqueness results for the solution of system (3) as follows [9]:

Theorem 2.1. *Let Ω be an open, bounded set of R^2 with $C^{1,1}$ boundary, and $g \in H^{1/2}(\Gamma_1)$. Then there exists at least one solution $(\mathbf{u}, p) \in \hat{V}_g(\Omega) \times \hat{M}(\Omega)$ of (3). Moreover, if $\nu > \nu_0(g)$ for some positive number ν_0 , then system (3) has a unique solution. Furthermore, if $g \in H^{3/2}(\Gamma_1)$, we can improve the regularity of the solution $(\mathbf{u}, p) \in (H^2(\Omega))^2 \times H^1(\Omega)$.*

Theorem 2.1 implies that the solution of (3) exists for any value of the Reynolds number. But the uniqueness can be guaranteed only for sufficiently large values of ν or for sufficiently small datum g .

The convergence result for the solution of the variational form (3) with respect to α is contained in the following theorem [9]:

Theorem 2.2. *Suppose that the conditions of Theorem 2.1 are satisfied. The solution of system (3) converges to the weak solution of the stationary incompressible Navier-Stokes equations without damping when α converges to zero.*

2.3. A shape optimization problem and adjoint equations. In this subsection, we are concerned with numerical methods for a shape optimization problem associated with flow governed by the stationary incompressible Navier-Stokes equations with damping. Our aim is to find an optimal shape Ω to minimize the total dissipative energy in the flow domain. In order to derive the shape gradient of the objective functional with respect to the domain, we shall need additional regularity for the solution of (3); i.e., $(\mathbf{u}, p) \in V_g(\Omega) \times M(\Omega)$ [11]. To achieve the needed smoothness, we will assume that all the conditions of Theorem 2.1 are satisfied in the rest of this paper.

We define the set of admissible domains

$$Q_{ad} = \{\Omega \subset U \mid \Omega \text{ with piecewise } C^{1,1} \text{ boundary and } \Gamma_1 \cup \Gamma_2 \text{ is fixed}\}.$$

The shape optimization can be stated as

$$(4) \quad \begin{aligned} \min_{\Omega \in Q_{ad}} J(\Omega) &= 2\nu \int_{\Omega} |e(\mathbf{u})|^2 dx, \\ \text{such that } (\mathbf{u}, p) &\in V_g(\Omega) \times M(\Omega) \text{ satisfies system (3),} \\ \int_{\Omega} dx &= C(\text{constant}), \end{aligned}$$

where $e(\mathbf{u}) = \frac{1}{2}(\nabla \mathbf{u} + (\nabla \mathbf{u})^T)$ is the deformation tensor for the velocity \mathbf{u} , and the objective functional represents the total dissipative energy in the flow domain.

Based on the control theory [11,15], system (2) is considered as a state constraint in the minimization problem. We construct a Lagrangian functional by introducing the so-called adjoint state variables (\mathbf{v}, q) and multiplier λ :

$$(5) \quad L(\Omega, \mathbf{u}, p, \mathbf{v}, q, \lambda) = J(\Omega) - F(\Omega, \mathbf{u}, p, \mathbf{v}, q) - V(\Omega, \lambda),$$

where

$$(6) \quad F(\Omega, \mathbf{u}, p, \mathbf{v}, q) = \int_{\Omega} [\nu \nabla \mathbf{u} : \nabla \mathbf{v} + (\mathbf{u} \cdot \nabla) \mathbf{u} \cdot \mathbf{v} + \alpha |\mathbf{u}|^{r-2} \mathbf{u} \cdot \mathbf{v} - p \operatorname{div} \mathbf{v}] dx - \int_{\Omega} \operatorname{div} \mathbf{u} q dx.$$

$$(7) \quad V(\Omega, \lambda) = \lambda \left(\int_{\Omega} dx - C \right).$$

Since

$$\max_{(\mathbf{v}, q) \in V_0(\Omega) \times M(\Omega)} \max_{\lambda \in R} L(\Omega, \mathbf{u}, p, \mathbf{v}, q, \lambda) = \begin{cases} J(\Omega) & \text{if } F(\Omega, \mathbf{u}, p, \mathbf{v}, q) = 0 \text{ and } V(\Omega, \lambda) = 0, \\ +\infty, & \text{if } F(\Omega, \mathbf{u}, p, \mathbf{v}, q) \neq 0 \text{ or } V(\Omega, \lambda) \neq 0, \end{cases}$$

then the solution of the shape optimization problem (4) is the minimum shape of the following saddle point problem:

$$\min_{\Omega \in Q_{ad}} \min_{(\mathbf{u}, p) \in V_g(\Omega) \times M(\Omega)} \max_{(\mathbf{v}, q) \in V_0(\Omega) \times M(\Omega)} \max_{\lambda \in R} L(\Omega, \mathbf{u}, p, \mathbf{v}, q, \lambda)$$

Setting the first variation of L with respect to the Lagrange multiplier λ and the adjoint variable (\mathbf{v}, q) to zero is equivalent to the condition to maintain a constant volume and the stationary Navier-Stokes equations with damping (2).

Setting the first variation of L with respect to the state variable p in the arbitrary direction $\tilde{p} \in M(\Omega)$ to zero is equivalent to the condition

$$\frac{\partial L}{\partial p}(\Omega, \mathbf{u}, p, \mathbf{v}, q, \lambda) \cdot \tilde{p} = \int_{\Omega} \tilde{p} \operatorname{div} \mathbf{u} \, dx = 0.$$

Since the variation \tilde{p} is arbitrary, we obtain

$$(8) \quad \operatorname{div} \mathbf{v} = 0$$

Setting the first variation of L with respect to the state variable \mathbf{u} in the arbitrary direction $\tilde{\mathbf{u}} \in V_0(\Omega)$ to zero is equivalent to the following condition (and using Green's formula and divergence free condition (8)):

$$\begin{aligned} 0 &= \frac{\partial L}{\partial \mathbf{u}}(\Omega, \mathbf{u}, p, \mathbf{v}, q, \lambda) \cdot \tilde{\mathbf{u}} \\ &= 4\nu \int_{\Omega} e(\mathbf{u}) : e(\tilde{\mathbf{u}}) \, dx \\ &\quad - \int_{\Omega} [\nu \nabla \tilde{\mathbf{u}} : \nabla \mathbf{v} + (\tilde{\mathbf{u}} \cdot \nabla) \mathbf{u} \cdot \mathbf{v} + (\mathbf{u} \cdot \nabla) \tilde{\mathbf{u}} \cdot \mathbf{v} + \int_{\Omega} \operatorname{div} \tilde{\mathbf{u}} q] \, dx \\ &\quad - \int_{\Omega} [\alpha |\mathbf{u}|^{r-2} \tilde{\mathbf{u}} + \alpha(r-2) |\mathbf{u}|^{r-4} (\mathbf{u} \cdot \tilde{\mathbf{u}}) \mathbf{u}] \cdot \mathbf{v} \, dx \\ &= \int_{\Omega} [-4\nu \operatorname{div} e(\mathbf{u}) + \nu \Delta \mathbf{v} - (\nabla \mathbf{u})^T \cdot \mathbf{v} + (\mathbf{u} \cdot \nabla) \mathbf{v} \\ &\quad - (\alpha |\mathbf{u}|^{r-2} \mathbf{v} + \alpha(r-2) |\mathbf{u}|^{r-4} (\mathbf{u} \cdot \mathbf{v}) \mathbf{u} - \nabla q] \cdot \tilde{\mathbf{u}} \, dx \\ &\quad + \int_{\Gamma_2} [4\nu e(\mathbf{u}) \cdot \mathbf{n} - (\nu \frac{\partial \mathbf{v}}{\partial \mathbf{n}} + (\mathbf{u} \cdot \mathbf{n}) \mathbf{v} - \mathbf{n} q)] \cdot \tilde{\mathbf{u}} \, ds \end{aligned}$$

First, taking an arbitrary variation $\tilde{\mathbf{u}}$ which vanishes in a neighborhood of the boundary Γ_2 , we have

$$(9) \quad -\nu \Delta \mathbf{v} + (\nabla \mathbf{u})^T \cdot \mathbf{v} - (\mathbf{u} \cdot \nabla) \mathbf{v} + \alpha |\mathbf{u}|^{r-4} (|\mathbf{u}|^2 \mathbf{v} + (r-2)(\mathbf{u} \cdot \mathbf{v}) \mathbf{u}) + \nabla q = -2\nu \Delta \mathbf{u}.$$

Next, taking an arbitrary $\tilde{\mathbf{u}}$ in Γ_2 gives

$$(10) \quad \nu \frac{\partial \mathbf{v}}{\partial \mathbf{n}} + (\mathbf{u} \cdot \mathbf{n}) \mathbf{v} - \mathbf{n} q = 4\nu e(\mathbf{u}) \cdot \mathbf{n} \quad \text{on } \Gamma_2$$

Finally, the adjoint equations are obtained

$$(11) \quad \left\{ \begin{array}{ll} -\nu \Delta \mathbf{v} + (\nabla \mathbf{u})^T \cdot \mathbf{v} - (\mathbf{u} \cdot \nabla) \mathbf{v} + \alpha |\mathbf{u}|^{r-4} (|\mathbf{u}|^2 \mathbf{v} \\ \quad + (r-2)(\mathbf{u} \cdot \mathbf{v}) \mathbf{u}) + \nabla q = -4\nu \operatorname{div} e(\mathbf{u}), & \text{in } \Omega, \\ \operatorname{div} \mathbf{v} = 0, & \text{in } \Omega, \\ \mathbf{v} = 0, & \text{on } \Gamma_0 \cup \Gamma_1, \\ \nu \frac{\partial \mathbf{v}}{\partial \mathbf{n}} + (\mathbf{u} \cdot \mathbf{n}) \mathbf{v} - \mathbf{n} q = 4\nu e(\mathbf{u}) \cdot \mathbf{n}, & \text{on } \Gamma_2, \end{array} \right.$$

The adjoint equations are linear equations with mixed boundary conditions. Their variational form reads as

$$(12) \quad \left\{ \begin{array}{l} \text{find } (\mathbf{v}, q) \in V_g(\Omega) \times M(\Omega) \text{ such that} \\ \int_{\Omega} [\nu \nabla \mathbf{v} : \nabla \mathbf{w} + (\nabla \mathbf{u}) \cdot \mathbf{w} \cdot \mathbf{v} + \nabla \mathbf{w} \cdot \mathbf{u} \cdot \mathbf{v} \\ \quad + \alpha |\mathbf{u}|^{r-4} (|\mathbf{u}|^2 \mathbf{v} + (r-2)(\mathbf{u} \cdot \mathbf{v}) \mathbf{u}) \cdot \mathbf{w}] dx \\ \quad - \int_{\Omega} q \operatorname{div} \mathbf{w} dx = 4\nu \int_{\Omega} e(\mathbf{u}) : e(\mathbf{w}) dx, \quad \forall \mathbf{w} \in V_0(\Omega), \\ \int_{\Omega} \operatorname{div} \mathbf{v} \psi dx = 0, \quad \forall \psi \in M(\Omega). \end{array} \right.$$

2.4. Shape gradient. In this subsection, we will derive the shape gradient of the saddle point formulation by a function space parametrization technique.

As the boundaries Γ_1 and Γ_2 are fixed in the admissible set of domains, we define the velocity field in the velocity method as follows:

$$V_{ad} = \{\mathbf{V} \in C^0(0, \tau; (C^2(\mathbb{R}^2))^2) \mid \mathbf{V} = 0 \quad \text{on } \Gamma_1 \cup \Gamma_2\}.$$

Under the action of velocity V for $t \geq 0$, the domain Ω is transformed into a domain $\Omega_t = T_t(\Omega)$ by the velocity method with formulation (1). Now, we need to state an expression for the derivative of the saddle point problem $j(t)$ with respect to t , where

$$j(t) = \min_{(\mathbf{u}_t, p_t) \in V_g(\Omega_t) \times M(\Omega_t)} \max_{(\mathbf{v}_t, q_t) \in V_0(\Omega_t) \times M(\Omega_t)} \max_{\lambda \in \mathbb{R}} L(\Omega_t, \mathbf{u}_t, p_t, \mathbf{v}_t, q_t, \lambda),$$

(\mathbf{u}_t, p_t) and (\mathbf{v}_t, q_t) are the solutions of the state equations (2) and the adjoint equations (11) in the perturbed domain Ω_t , respectively. Next, we utilize the following function space parametrization technique to avoid the difficulty brought by the Hilbert space $V_g(\Omega_t)$, $V_0(\Omega_t)$ and $M(\Omega_t)$ which all depend on the parameter t :

$$\begin{aligned} V_0(\Omega_t) &= \{\mathbf{u} \circ T_t^{-1} : \mathbf{u} \in V_0(\Omega)\}; \\ V_g(\Omega_t) &= \{\mathbf{u} \circ T_t^{-1} : \mathbf{u} \in V_g(\Omega)\}; \\ M(\Omega_t) &= \{p \circ T_t^{-1} : p \in M(\Omega)\}; \end{aligned}$$

This parametrization do not influence the value of the saddle point $j(t)$ because T_t and T_t^{-1} are diffeomorphisms. We have

$$j(t) = \min_{(\mathbf{u}, p) \in V_g(\Omega) \times M(\Omega)} \max_{(\mathbf{v}, q) \in V_0(\Omega) \times M(\Omega)} \max_{\lambda \in \mathbb{R}} L(\Omega_t, \mathbf{u} \circ T_t^{-1}, p \circ T_t^{-1}, \mathbf{v} \circ T_t^{-1}, q \circ T_t^{-1}, \lambda).$$

Note that the Lagrangian functional is

$$L(\Omega_t, \mathbf{u} \circ T_t^{-1}, p \circ T_t^{-1}, \mathbf{v} \circ T_t^{-1}, q \circ T_t^{-1}, \lambda) = l_1(t) - l_2(t) - l_3(t),$$

where

$$\begin{aligned} l_1(t) &= 2\nu \int_{\Omega_t} |e(\mathbf{u} \circ T_t^{-1})|^2 dx, \\ l_2(t) &= \int_{\Omega_t} [\nu \nabla(\mathbf{u} \circ T_t^{-1}) : \nabla(\mathbf{v} \circ T_t^{-1}) + ((\mathbf{u} \circ T_t^{-1}) \cdot \nabla)(\mathbf{u} \circ T_t^{-1}) \cdot (\mathbf{v} \circ T_t^{-1}) \\ &\quad + \alpha |\mathbf{u} \circ T_t^{-1}|^{r-2} (\mathbf{u} \circ T_t^{-1}) \cdot (\mathbf{v} \circ T_t^{-1}) - (p \circ T_t^{-1}) \operatorname{div}(\mathbf{v} \circ T_t^{-1})] dx \\ &\quad - \int_{\Omega_t} \operatorname{div}(\mathbf{u} \circ T_t^{-1})(q \circ T_t^{-1}) dx, \\ l_3(t) &= \lambda \left(\int_{\Omega_t} dx - C \right) \end{aligned}$$

If $f : [0, \tau] \times R^2 \rightarrow R$ is sufficiently smooth, we have the following formula[23]:

$$(13) \quad \frac{d}{dt} \int_{\Omega_t} f(t, x) dx|_{t=0} = \int_{\Omega} \frac{\partial f}{\partial t}(0, x) dx + \int_{\partial\Omega} f(0, x) \mathbf{V}(0, X) \cdot \mathbf{n} ds.$$

Let $\mathbf{V}(0, X) \in V_{ad}$, and Note that $\mathbf{V}(0, X) = \mathbf{V}$. Then we can compute the shape gradient with formula (13):

$$(14) \quad \frac{d}{dt} L(\Omega_t, \mathbf{u} \circ T_t^{-1}, p \circ T_t^{-1}, \mathbf{v} \circ T_t^{-1}, q \circ T_t^{-1}, \lambda)|_{t=0} = l'_1(0) - l'_2(0) - l'_3(0),$$

where

$$\begin{aligned} l'_1(0) &= 4\nu \int_{\Omega} e(\mathbf{u}) : e(-\nabla \mathbf{u} \cdot \mathbf{V}) d\Omega + 2\nu \int_{\Gamma_0} (|e(\mathbf{u})|^2 \mathbf{V} \cdot \mathbf{n}) ds, \\ l'_2(t) &= \int_{\Omega} [\nu \nabla(-\nabla \mathbf{u} \cdot \mathbf{V}) : \nabla \mathbf{v} + \nu \nabla(\mathbf{u}) : \nabla(-\nabla \mathbf{v} \cdot \mathbf{V}) \\ &\quad + ((-\nabla \mathbf{u} \cdot \mathbf{V}) \cdot \nabla \mathbf{u}) \cdot \mathbf{v} + (\mathbf{u} \cdot \nabla(-\nabla \mathbf{u} \cdot \mathbf{V})) \cdot \mathbf{v} + (\mathbf{u} \cdot \nabla \mathbf{u}) \cdot (-\nabla \mathbf{v} \cdot \mathbf{V}) \\ &\quad + \alpha(r-2)|\mathbf{u}|^{r-4}(-\nabla \mathbf{u} \cdot \mathbf{V} \cdot \mathbf{u})(\mathbf{u} \cdot \mathbf{v}) + \alpha|\mathbf{u}|^{r-2}(-\nabla \mathbf{u} \cdot \mathbf{V}) \cdot \mathbf{v} \\ &\quad + \alpha|\mathbf{u}|^{r-2} \mathbf{u} \cdot (-\nabla \mathbf{v} \cdot \mathbf{V}) - (\nabla p \cdot \mathbf{V}) \operatorname{div}(\mathbf{v}) \\ &\quad - p \operatorname{div}(-\nabla \mathbf{v} \cdot \mathbf{V}) - \operatorname{div}(-\nabla \mathbf{u} \cdot \mathbf{V}) q - \operatorname{div}(\mathbf{u})(-\nabla q \cdot \mathbf{V})] dx, \\ &\quad + \int_{\Gamma_0} [\nu \nabla \mathbf{u} : \nabla \mathbf{v} + (\mathbf{u} \cdot \nabla \mathbf{u}) \cdot \mathbf{v} \\ &\quad + \alpha|\mathbf{u}|^{r-2} \mathbf{u} \cdot \mathbf{v} - p \operatorname{div} \mathbf{v} - \operatorname{div} \mathbf{u} q] \mathbf{V} \cdot \mathbf{n} ds, \\ l'_3(t) &= \lambda \int_{\Gamma_0} \mathbf{V} \cdot \mathbf{n} ds. \end{aligned}$$

Employing Green's formula and the fact that \mathbf{u} vanishes on Γ_0 , we have

$$(16) \quad \begin{aligned} l'_2(t) &= - \int_{\Omega} [(-\nu \Delta \mathbf{u} + (\mathbf{u} \cdot \nabla) \mathbf{u} + \nabla p) \cdot (\nabla \mathbf{v} \cdot \mathbf{V})] dx + \int_{\Omega} \operatorname{div} \mathbf{u} (\nabla q \cdot \mathbf{V}) dx \\ &\quad + \int_{\Omega} \operatorname{div} \mathbf{v} (\nabla p \cdot \mathbf{V}) dx + \int_{\Omega} [-\nu \Delta \mathbf{v} + (\nabla \mathbf{u})^T \cdot \mathbf{v} - (\mathbf{u} \cdot \nabla) \mathbf{v} \\ &\quad + \alpha|\mathbf{u}|^{r-4}(|\mathbf{u}|^2 \mathbf{v} + (r-2)(\mathbf{u} \cdot \mathbf{v}) \mathbf{u}) - \nabla q] \cdot (\nabla \mathbf{u} \cdot \mathbf{V})] dx \\ &\quad - \int_{\Gamma_0} [\nu \frac{\partial \mathbf{v}}{\partial \mathbf{n}} + (\mathbf{u} \cdot \mathbf{n}) \mathbf{v} - \mathbf{n} q] \cdot (\nabla \mathbf{u} \cdot \mathbf{V}) ds - \int_{\Gamma_0} [\nu \frac{\partial \mathbf{u}}{\partial \mathbf{n}} - \mathbf{n} p] \cdot (\nabla \mathbf{v} \cdot \mathbf{V}) ds \\ &\quad + \int_{\Gamma_0} [\nu \nabla \mathbf{u} : \nabla \mathbf{v} + (\mathbf{u} \cdot \nabla \mathbf{u}) \cdot \mathbf{v} + \alpha|\mathbf{u}|^{r-2}(\mathbf{u} \cdot \mathbf{v}) - p \operatorname{div} \mathbf{v} - \operatorname{div} \mathbf{u} q] \mathbf{V} \cdot \mathbf{n} ds \end{aligned}$$

$$(17) \quad l'_3(t) = \lambda \int_{\Gamma_0} \mathbf{V} \cdot \mathbf{n} ds.$$

We substitute (15), (16) and (17) into (14), and note that (\mathbf{u}, p) and (\mathbf{v}, q) satisfy (2) and (11), respectively, to obtain the shape derivative

$$(18) \quad \begin{aligned} dJ(\Omega; \mathbf{V}) &= \frac{d}{dt} L|_{t=0} \\ &= -2\nu \int_{\Gamma_0} (|e(\mathbf{u})|^2 \mathbf{V} \cdot \mathbf{n}) ds + \int_{\Gamma_0} [\nu \frac{\partial \mathbf{v}}{\partial \mathbf{n}} + \mathbf{n} q] \cdot (\nabla \mathbf{u} \cdot \mathbf{V}) ds \\ &\quad + \int_{\Gamma_0} [\nu \frac{\partial \mathbf{u}}{\partial \mathbf{n}} - \mathbf{n} p] \cdot (\nabla \mathbf{v} \cdot \mathbf{V}) ds - \int_{\Gamma_0} [(\nu \nabla \mathbf{u} : \nabla \mathbf{v}) \mathbf{V} \cdot \mathbf{n} ds \\ &\quad - \lambda \int_{\Gamma_0} \mathbf{V} \cdot \mathbf{n} ds. \end{aligned}$$

Since $\mathbf{u} = \mathbf{v} = 0$ in Γ_0 , we have

$$(19) \quad n \cdot (\nabla \mathbf{u} \cdot \mathbf{V}) = \nabla \mathbf{u} \cdot (\mathbf{n} \otimes \mathbf{n}) \cdot \mathbf{V} \cdot \mathbf{n} = \nabla \mathbf{u} \cdot \mathbf{n} \cdot \mathbf{n} (\mathbf{V} \cdot \mathbf{n}) = \operatorname{div} \mathbf{u} (\mathbf{V} \cdot \mathbf{n}) = 0, \quad \forall x \in \Gamma_0$$

$$(20) \quad \frac{\partial \mathbf{v}}{\partial \mathbf{n}} \cdot (\nabla \mathbf{u} \cdot \mathbf{V}) = \nabla \mathbf{u} \cdot (\mathbf{n} \otimes \mathbf{n}) \cdot \mathbf{V} \cdot \frac{\partial \mathbf{v}}{\partial \mathbf{n}} = \frac{\partial \mathbf{u}}{\partial \mathbf{n}} \cdot \frac{\partial \mathbf{v}}{\partial \mathbf{n}} (\mathbf{V} \cdot \mathbf{n}) = (\nabla \mathbf{u} : \nabla \mathbf{v}) \mathbf{V} \cdot \mathbf{n}$$

Similarly, we see that

$$(21) \quad \mathbf{n} \cdot (\nabla \mathbf{v} \cdot \mathbf{V}) = 0, \quad \frac{\partial \mathbf{u}}{\partial \mathbf{n}} \cdot (\nabla \mathbf{v} \cdot \mathbf{V}) = \frac{\partial \mathbf{u}}{\partial \mathbf{n}} \cdot \frac{\partial \mathbf{v}}{\partial \mathbf{n}} (\mathbf{V} \cdot \mathbf{n}) = (\nabla \mathbf{u} : \nabla \mathbf{v}) \mathbf{V} \cdot \mathbf{n}.$$

According to (19), (20), and (21), the shape derivative (18) can be simplified as follows:

$$(22) \quad dJ(\Omega; \mathbf{V}) = \int_{\Gamma_0} [-2\nu|e(\mathbf{u})|^2 + \nu \frac{\partial \mathbf{u}}{\partial \mathbf{n}} \cdot \frac{\partial \mathbf{v}}{\partial \mathbf{n}} - \lambda] \mathbf{V} \cdot \mathbf{n} \, ds.$$

Therefore, the expression of the shape gradient can be given by

$$(23) \quad \nabla J = [-2\nu|e(\mathbf{u})|^2 + \nu \frac{\partial \mathbf{u}}{\partial \mathbf{n}} \cdot \frac{\partial \mathbf{v}}{\partial \mathbf{n}} - \lambda] \mathbf{n}.$$

We assume that $\nabla J = 0$; then the first-order optimality condition of the shape optimization problem is obtained by

$$(24) \quad -2\nu|e(\mathbf{u})|^2 + \nu \frac{\partial \mathbf{u}}{\partial \mathbf{n}} \cdot \frac{\partial \mathbf{v}}{\partial \mathbf{n}} - \lambda = 0.$$

Finally, the optimality system is composed of the condition $\int_{\Omega} dx = C$, formula (24), state equations (2), and adjoint equations(11). Of course, one needs to solve this system to obtain the optimal shape. We will solve this shape optimization problem with a gradient-based method, since the optimality system is a nonlinear large-scale problem.

3. An adaptive finite element method

3.1. Finite element discretization. For the finite element discretization, let K_h be a regular triangulation of the domain Ω , indexed by a parameter $h = \max_{K \in K_h} \{\text{diam}(K)\}$. We choose the finite element subspaces $V_{0h} \subset V_0$, $V_{gh} \subset V_g$, and $M_h \subset M$ as follows:

$$\begin{aligned} V_{0h} &= \{\mathbf{v}_h \in C(\Omega)^2; \mathbf{v}_h|_K \in P_2(K)^2, \forall K \in K_h, \mathbf{v}_h = 0 \text{ on } \Gamma_0 \cup \Gamma_1\}, \\ V_{gh} &= \{\mathbf{v}_h \in C(\Omega)^2; \mathbf{v}_h|_K \in P_2(K)^2, \forall K \in K_h, \mathbf{v}_h = 0 \text{ on } \Gamma_0, \mathbf{v}_h = g \text{ on } \Gamma_1\}, \\ M_h &= \{p_h \in C(\Omega); p_h|_K \in P_1(K), \forall K \in K_h\}, \end{aligned}$$

where $P_k(K)$ ($k = 1, 2$) is the space of piecewise polynomials of degree k on K . We will also need the piecewise constant space

$$R_0 = \{l_h \in L^2(\Omega) : l_h|_K \in P_0(K) \quad \forall K \in K_h\}.$$

It is obvious that (V_{0h}, M_h) , (V_{gh}, M_h) satisfies the discrete LBB condition [10]:

$$(25) \quad \sup_{0 \neq \mathbf{v}_h \in V_h} \frac{\int q_h \text{div} \mathbf{v}_h \, dx}{\|\mathbf{v}_h\|_1} \geq \beta \|q_h\|_0, \quad \forall q_h \in M_h, V_h = V_{0h} \text{ or } V_{gh}.$$

The Galerkin finite element discretizations of the state equations (3) and the adjoint equations (12) in the $P_2 - P_1$ element pair are as follows:

$$(26) \quad \begin{cases} \text{find } (\mathbf{u}_h, p_h) \in V_{gh} \times M_h \text{ such that} \\ \int_{\Omega} [\nu \nabla \mathbf{u}_h : \nabla \mathbf{v}_h + (\mathbf{u}_h \cdot \nabla) \mathbf{u}_h \cdot \mathbf{v}_h + \alpha |\mathbf{u}_h|^{r-2} \mathbf{u}_h \cdot \mathbf{v}_h \\ \quad \quad \quad - p_h \text{div} \mathbf{v}_h] \, dx = 0, & \forall \mathbf{v}_h \in V_{0h}, \\ \int_{\Omega} \text{div} \mathbf{u}_h q_h \, dx = 0, & \forall q_h \in M_h. \end{cases}$$

and

$$(27) \quad \left\{ \begin{array}{l} \text{find } (\mathbf{v}_h, q_h) \in V_{gh} \times M_h \text{ such that} \\ \int_{\Omega} [\nu \nabla \mathbf{v}_h : \nabla \mathbf{w}_h + (\nabla \mathbf{u}_h) \cdot \mathbf{w}_h \cdot \mathbf{v}_h + \nabla \mathbf{w}_h \cdot \mathbf{u}_h \cdot \mathbf{v}_h \\ \quad + \alpha |\mathbf{u}_h|^{r-4} (|\mathbf{u}_h|^2 \mathbf{v}_h + (r-2)(\mathbf{u}_h \cdot \mathbf{v}_h) \mathbf{u}_h) \cdot \mathbf{w}_h] dx \\ \quad + \int_{\Omega} q_h \operatorname{div} \mathbf{w}_h dx = 4\nu \int_{\Omega} e(\mathbf{u}_h) : e(\mathbf{w}_h) dx, \quad \forall \mathbf{w}_h \in V_{0h}, \\ \int_{\Omega} \operatorname{div} \mathbf{v}_h \psi dx = 0, \quad \forall \psi \in M_h. \end{array} \right.$$

The functional $J(\Omega)$ is approximated by

$$J_h(\Omega) = 2\nu \int_{\Omega} |e(\mathbf{u}_h)|^2 dx.$$

Next, we will introduce a regularized method for the shape gradient (23) to avoid the boundary oscillation brought by the less regularity [22]. The main idea of this method is to find a

$$(28) \quad \left\{ \begin{array}{l} -\Delta \mathbf{d} + \mathbf{d} = 0 \quad \text{in } \Omega, \\ \mathbf{d} = 0, \quad \text{on } \Gamma_1 \cup \Gamma_2, \\ \frac{\partial \mathbf{d}}{\partial \mathbf{n}} = -\nabla J, \quad \text{on } \Gamma_0. \end{array} \right.$$

Note that

$$V_d(\Omega) = \{\mathbf{v} \in (H^1(\Omega))^2 \mid \mathbf{v} = 0 \text{ on } \Gamma_1 \cup \Gamma_2\},$$

$$V_{dh} = \{\mathbf{v}_h \in C(\Omega)^2; \mathbf{v}_h|_K \in P_2(K)^2, \forall K \in K_h, \mathbf{v}_h = 0 \text{ on } \Gamma_1 \cup \Gamma_2\}.$$

The weak form of formula (28) is given as follows:

$$(29) \quad \left\{ \begin{array}{l} \text{find } \mathbf{d} \in V_d(\Omega) \text{ such that} \\ \int_{\Omega} [\nu \nabla \mathbf{d} : \nabla \mathbf{w} + \mathbf{d} \cdot \mathbf{w}] dx = \int_{\Gamma_0} (-\nabla J) \cdot \mathbf{w} ds, \quad \forall \mathbf{w} \in V_{dh}(\Omega). \end{array} \right.$$

and the Galerkin approximating is

$$(30) \quad \left\{ \begin{array}{l} \text{find } \mathbf{d}_h \in V_{dh} \text{ such that} \\ \int_{\Omega} [\nu \nabla \mathbf{d}_h : \nabla \mathbf{w}_h + \mathbf{d}_h \cdot \mathbf{w}_h] dx = \int_{\Gamma_0} (-\nabla J) \cdot \mathbf{w} ds, \quad \forall \mathbf{w} \in V_d(\Omega). \end{array} \right.$$

Now, we state the algorithm as follows: Start with an initial shape Ω_0 , an initial step ρ_0 and a Lagrange multiplier λ_0 . For $m = 0, 1, 2, \dots$, until a stopping criterion is achieved,

1. Solve the state equations (26) to obtain the corresponding (\mathbf{u}^m, p^m) .
 2. Solve the adjoint equations (27) to obtain the adjoint variable (\mathbf{v}^m, q^m) .
 3. Solve equations (30) to get a regularized gradient direction \mathbf{d}^m .
 4. Compute $\Omega_{m+1} = \Omega_m + \rho_m \mathbf{d}^m$ and refresh the Lagrange multiplier λ_{m+1} .
- The Lagrange multiplier in Step 4 can be computed as follows:

$$\lambda_{m+1} = (\lambda_m - \frac{\int_{\Gamma_0} (-2\nu |e(\mathbf{u})|^2 + \nu \frac{\partial \mathbf{u}}{\partial \mathbf{n}} \cdot \frac{\partial \mathbf{v}}{\partial \mathbf{n}}) ds}{\int_{\Gamma_0} ds}) / 2 + \gamma |V(\Omega_m) - V_{\text{target}}(\Omega)| / V_{\text{target}}(\Omega),$$

where $V_{\text{target}}(\Omega)$ denotes the target volume of the shape and γ is a small positive number.

3.2. Projection error estimation and adaptivity. In this subsection, we will present an adaptive finite element method based on an a-posteriori error estimator constructed by projection for the state, adjoint and regularized gradient equations. This method is motivated by the stabilized finite element method based on the two local Gauss integrals technique in recent years [19-21,24,25]. Before deriving the a-posteriori estimator, we define the orthogonal projection operator $\Pi : L^2(\Omega) \rightarrow R_0$ which satisfies the following properties:

$$\begin{aligned} ((I - \Pi)\psi, l_h) &= 0 \quad \forall \psi \in L^2(\Omega), l_h \in R_0, \\ \|\Pi\psi\|_0 &\leq C\|\psi\|_0 \quad \forall \psi \in L^2(\Omega), \\ \|(I - \Pi)\psi\|_0 &\leq Ch\|\psi\|_1 \quad \forall \psi \in H^1(\Omega). \end{aligned}$$

Here, I is the identity operator. In the following discussion, the operators $\Pi^{2 \times 2}$ and $\Pi^{2 \times 1}$, which act on the velocity deformation tensor and the gradient of the regularized function $\nabla \mathbf{d}_h$, respectively, are also denoted by Π for simplicity.

Now, based on the residual between the gradient of the finite element solution velocity component $\nabla \mathbf{u}_h$, the regularized function $\nabla \mathbf{d}_h$, the pressure component p_h , and their projections $\Pi \nabla \mathbf{u}_h$, $\Pi \nabla p_h$, and $\Pi \nabla \mathbf{d}_h$, the a-posteriori estimator can be constructed locally as follows:

$$(30) \quad \eta_{\Pi, K} := \|(I - \Pi)\nabla \mathbf{u}_h\|_{0, K} + \|(I - \Pi)p_h\|_{0, K} + \|(I - \Pi)\nabla \mathbf{d}_h\|_{0, K}.$$

Then the global error estimator is given by

$$\eta := \left(\sum_{K \in K_h} \eta_{\Pi, K}^2 \right)^{\frac{1}{2}}$$

Based on the orthogonal projection properties of operator Π , the local projection error estimator can be computed more accurately and explicitly based on the two local Gauss integrals technique presented in [19-21]. Before giving a global upper bound, we recall a lemma in [29].

Lemma 3.1. *There exists a positive constant C such that*

$$(31) \quad Ch\|\nabla p_h\|_0 \leq \|(I - \Pi)p_h\|_0 \quad \forall p_h \in M_h.$$

This lemma was stated in [29]; its proof will be rewritten here.

Proof. We note that p_h is continuous and Πp_h is constant on each element K from the definition of space M_h and the projection operator Π , so it is obvious that $\nabla(\Pi p_h)|_K = 0$.

Additionally, under some mild assumptions on K_h , the following inverse inequalities holds:

$$(32) \quad \|\nabla q_h\|_0 \leq C_I h^{-1} \|q_h\|_0, \quad q_h \in M_h.$$

For spaces concerned with vector-valued functions it will also hold.

As a result, using the above inverse inequality (32), we see that

$$\begin{aligned} h^2 \|\nabla p_h\|_0^2 &= \sum_{K \in K_h} h^2 \|\nabla p_h\|_{0, K}^2 = \sum_{K \in K_h} h^2 \|\nabla(I - \Pi)p_h\|_{0, K}^2 \\ &\leq \sum_{K \in K_h} C_I^2 \|(I - \Pi)p_h\|_{0, K}^2 \leq C \|(I - \Pi)p_h\|_0^2. \end{aligned}$$

Thus this completes the proof of Lemma 3.1.

For $\nabla \mathbf{u}_h \in R_1^{2 \times 2}$ and $\nabla \mathbf{d}_h \in R_1^{2 \times 2}$ (the spaces consisting of vector-valued functions), we have

$$(33) \quad Ch\|\nabla \mathbf{u}_h\|_1 \leq \|(I - \Pi)\nabla \mathbf{u}_h\|_0 \quad \forall \mathbf{u}_h \in V_{gh},$$

$$(34) \quad Ch\|\nabla \mathbf{d}_h\|_1 \leq \|(I - \Pi)\nabla \mathbf{d}_h\|_0 \quad \forall \mathbf{d}_h \in V_{dh}.$$

Theorem 3.1. *Suppose that there exist constants C_1, C_2 , and C_3 such that the solutions of (2), (26), (28) and (30) satisfy $0 < C_1 \leq \|p\|_1, \|p_h\|_1, \|\mathbf{u}\|_2, \|\nabla \mathbf{u}_h\|_1, \|\mathbf{d}\|_2, \|\nabla \mathbf{d}_h\|_1 \leq C_2$ and the non-degenerate property conditions $\|\nabla(\mathbf{u} - \mathbf{u}_h)\|_0 + \|p - p_h\|_0 \geq C_3 h$ and $\|\nabla(\mathbf{d} - \mathbf{d}_h)\| \geq C_3 h$ hold. Then we have the following global lower and upper bounds:*

$$(35) \quad \|\nabla(\mathbf{u} - \mathbf{u}_h)\|_0 + \|p - p_h\|_0 + \|\nabla(\mathbf{d} - \mathbf{d}_h)\|_0 \leq C\eta,$$

and

$$(36) \quad \eta \leq C(\|\nabla(\mathbf{u} - \mathbf{u}_h)\|_0 + \|p - p_h\|_0 + \|\mathbf{d} - \mathbf{d}_h\|_0),$$

where C_1, C_2, C_3 and C are independent of h .

Proof. The following result can be derived by the regularity of the solutions u, p, d , assumed conditions and the discussions of Lemma 3.1:

$$\begin{aligned} & \|\nabla(\mathbf{u} - \mathbf{u}_h)\|_0 + \|p - p_h\|_0 + \|\nabla(\mathbf{d} - \mathbf{d}_h)\|_0 \\ & \leq Ch\|\mathbf{u}\|_2 + Ch\|p\|_1 + Ch\|\mathbf{d}\|_2 \\ & \leq C\frac{C_2}{C_1}h\|\nabla \mathbf{u}_h\|_1 + C\frac{C_2}{C_1}h\|p_h\|_1 + C\frac{C_2}{C_1}h\|\nabla \mathbf{d}_h\|_1 \\ & \leq C(\|(I - \Pi)\nabla \mathbf{u}_h\|_0 + \|(I - \Pi)p_h\|_0 + \|(I - \Pi)\nabla \mathbf{d}_h\|_0) \\ & \leq C\eta. \end{aligned}$$

With the triangle inequality, the property of the projection operator, the regularity of the solutions and the assumed non-degenerate conditions, we have

$$\begin{aligned} \eta & = \|(I - \Pi)\nabla \mathbf{u}_h\|_0 + \|(I - \Pi)p_h\|_0 + \|(I - \Pi)\nabla \mathbf{d}_h\|_0 \\ & \leq \|(I - \Pi)\nabla \mathbf{u}\|_0 + \|(I - \Pi)\nabla(\mathbf{u} - \mathbf{u}_h)\|_0 + \|(I - \Pi)p\|_0 \\ & \quad + \|(I - \Pi)(p - p_h)\|_0 + \|(I - \Pi)\nabla \mathbf{d}\|_0 + \|(I - \Pi)\nabla(\mathbf{d} - \mathbf{d}_h)\|_0 \\ & \leq Ch\|\nabla u\|_1 + C\|\nabla(\mathbf{u} - \mathbf{u}_h)\|_0 + Ch\|p\|_1 + C\|p - p_h\|_0 \\ & \quad + Ch\|\nabla \mathbf{d}\|_1 + C\|\nabla(\mathbf{d} - \mathbf{d}_h)\|_0 \\ & \leq C(\|\nabla(\mathbf{u} - \mathbf{u}_h)\|_0 + \|p - p_h\|_0 + \|\nabla(\mathbf{d} - \mathbf{d}_h)\|_0), \end{aligned}$$

which finished the proof.

The a-posteriori error estimator (30) can be computed easily by the difference of two Gauss integrals, for example,

$$\|(I - \Pi)p_h\|_{0,K} = \left\{ \int_{K,n(n \geq 2)} p_h^2 dx - \int_{K,1} p_h^2 dx \right\}^{1/2},$$

where $\int_{K,n} p_h^2 dx$ and $\int_{K,1} p_h^2 dx$ represent numerical integrals of Gauss type with n points and one point, respectively, to approximate the value of $\int_K p_h^2 dx$.

4. Numerical results

In the first example, let $\alpha = 0$ in equations (2). We give the numerical simulation for the shape optimization in the steady incompressible flow without damping, the same as that in [26], and then compare the results between [26] and our method.

The flow is around a body D in a fixed rectangular domain $U = [-0.5, 1.5] \times [-0.5, 1.5]$ with a parabolic velocity $g(x, y) = (0.25 - y^2, 0)^T$ at the inlet, nonslip boundary conditions on the top, bottom and Γ_0 , and a free outflow condition on the outlet Γ_2 . The boundary Γ_0 of body S is to be optimized. The flow domain is $\Omega = U \setminus \bar{D}$, the boundary $\partial\Omega = \Gamma_0 \cup \Gamma_1 \cup \Gamma_2$ (see Figure 1). The initial shape of the body D is chosen to a circle with center $(0, 0)$ and radius $r = 0.3$. Our goal is to find a geometric shape of D whose volume is 0.1 to minimize the dissipative energy in the flow domain.

First, as the same as in [26], we denote $Err_{energy} = |J_{opt}(\Omega) - J_0(\Omega)|/|J_0(\Omega)|$ the proportion of the reduced dissipative energy, where $J_{opt}(\Omega)$ and $J_0(\Omega)$ present

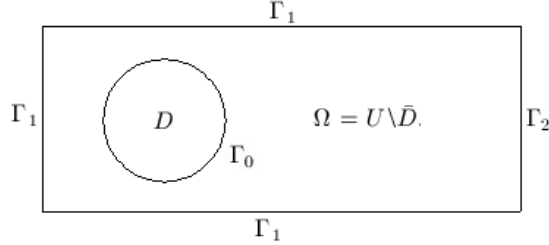


FIGURE 1. Domain and boundary

the values of the cost functional in the optimal shape and initial shape, respectively. We also denote the optimal shape as V_{opt} . Method I in Tables 1 and 2 is the method used in [26] which adopts the Zienkiewica-Zhu recovery procedure to refine the mesh adaptively. Method II is the adaptive finite element method based on the projection posteriori presented here. From Tables 1 and 2, when the objective functional achieves almost the same level accuracy, our method needs a fewer number of iterations than the method in [26]. The CPU time can be as much as 1/4 of that required in [26]. Hence our method converges much faster than the method given in [26].

TABLE 1. Results for the two methods with $Re = 200$

Method	Numbers of iterations	Err_{energy}	$V_{opt}(\Omega)$	CPU time
I	30	0.814348	1.91777	1247.43
II	21	0.814013	1.91835	978.271

TABLE 2. Results for the two methods with $Re = 400$

Method	Numbers of iterations	Err_{energy}	$V_{opt}(\Omega)$	CPU time
I	42	0.82673	1.91796	2450.95
II	28	0.825999	1.91919	1840.75

Figures 3 -12 give the comparisons between Methods I and II in terms of the shape and mesh at different iteration step. There is interesting phenomenon found in these figures. At each first iteration step, Method II generates much fewer grids than Method I, but it converges faster than Method I. Relative to Method I, Method II does not always refine its mesh in the domain in which flow changes quickly at the beginning (see Figures 6 and 7). Method II pursues a balance of the error between the state variable and the regularized variable which determines the accuracy of the shape gradient at each iteration step. Thus the a-posteriori estimator given here is a goal-oriented error estimation. Another observation is that the meshes generated by Method I are distorted in the optimization process although it uses the same initial mesh as Method II in Figure 2. Method II generates a more regular mesh than Method I, and can obtain a more accurate shape gradient in every optimal cycle. Therefore, Method II can achieve the the same optimal shape (see Figures 11 and 12) with a fewer number of iteration steps than Method I.

In the second example, we will consider the shape optimization problem in stationary incompressible flow with damping. The external domain and the boundary

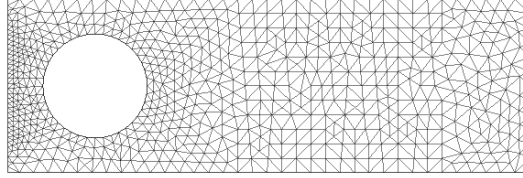


FIGURE 2. The initial mesh in method I and II

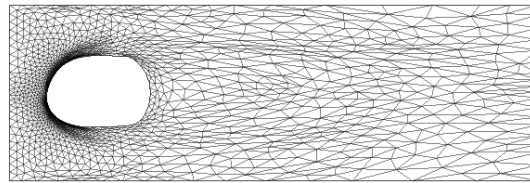


FIGURE 3. Finite element mesh at iteration 5 in method I (Re=300)

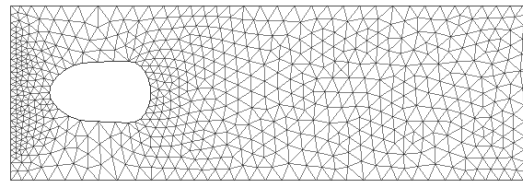


FIGURE 4. Finite element mesh at iteration 5 in method II (Re=300)

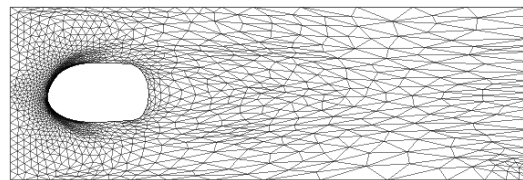


FIGURE 5. Finite element mesh at iteration 10 in method I (Re=300)

conditions are chosen the same as in example one. We only change the area for the admissible set of shapes as follows:

$$Q_{ad} = \{\Gamma_1 \cup \Gamma_2 \text{ is fixed, and the area } V_{\text{target}}(\Omega) = 1.93\},$$

which means that the target area of body D to be optimized is 0.7.

We choose NACA0040 to be the initial shape of the body, and Figure 13 is the initial computational mesh. The parameters in the damping term in equations (2) are taken by $\alpha = 10^{-4}$ and $r = 3$. Figure 14 gives the optimal shape with $Re = 400$.

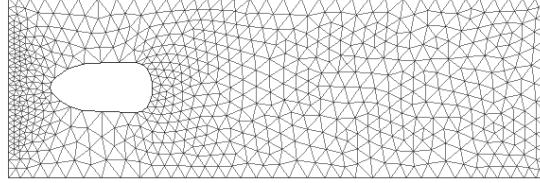


FIGURE 6. Finite element mesh at iteration 10 in method II(Re=300)

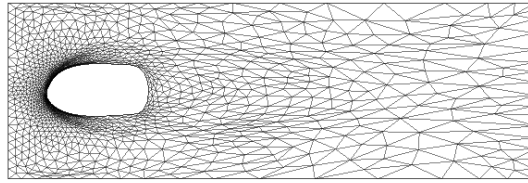


FIGURE 7. Finite element mesh at iteration 15 in method I(Re=300)

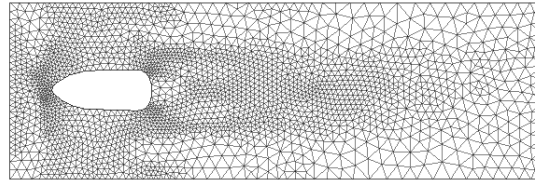


FIGURE 8. Finite element mesh at iteration 15 in method II (Re=300)

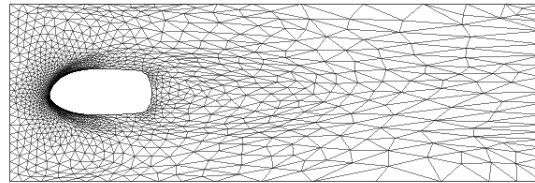


FIGURE 9. Finite element mesh at iteration 20 in method I(Re=300)

The distributions of the pressure and horizontal velocity for the optimal shape are giving by Figures 15 and 16, respectively.

5. Conclusions

An adaptive finite element method based on an a-posteriori error estimator is developed to solve a shape optimization problem in stationary incompressible flow in two dimensions. The error estimator is constructed by a projection operator, and can be obtained by the difference of two local Gauss integrals. It can be

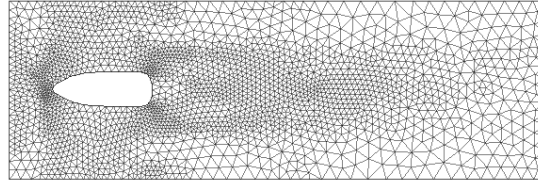


FIGURE 10. Finite element mesh at iteration 20 in method II ($Re=300$)

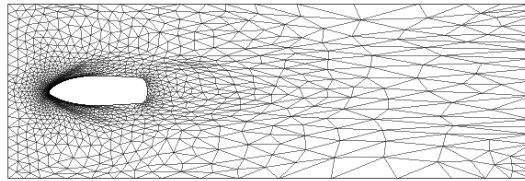


FIGURE 11. Finite element mesh for optimal shape in method I ($Re=300$)

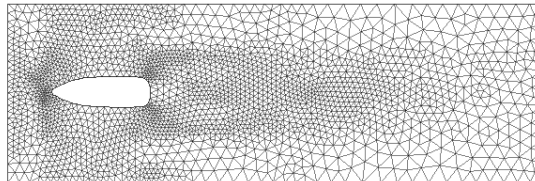


FIGURE 12. Finite element mesh for optimal shape in method II ($Re=300$)

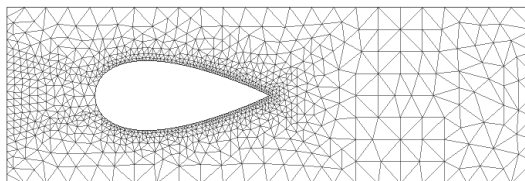


FIGURE 13. The initial domain and mesh

computed explicitly and quickly. More importantly, our error estimator balances the accuracy between the state variable, adjoint variable and regularized variable so that it converges quickly in the solution of the optimal problem governed by partial differential equations. In addition, this method can be also extended to solve free boundary problems.

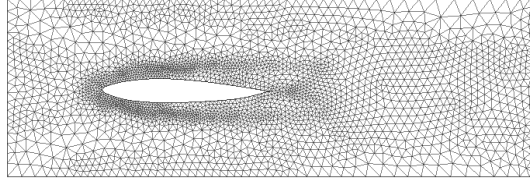


FIGURE 14. Finite element mesh for optimal shape (Re=400)

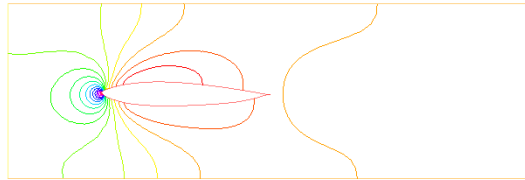


FIGURE 15. Distribution of the pressure for the optimal shape (Re=400)

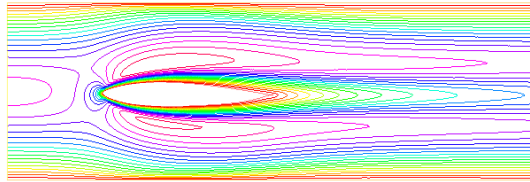


FIGURE 16. Distribution of the horizontal velocity for the optimal shape (Re=400)

References

- [1] I. Babuška and W.C. Rheinboldt, Error estimates for adaptive finite element computations, *SIAM J. Numer. Anal.*, 15 (1978), pp. 736-754.
- [2] Wenbin Liu and Ningning Yan, A posteriori error estimates for control problems governed by Stokes equations, *SIAM J. Numer. Anal.*, Vol. 40, No. 5, pp. 1850-1869, 2002.
- [3] Wolfgang Bangerth, A framework for the adaptive finite element solution of large-scale inverse problems, *SIAM J. SCI. Comput.*, Vol. 30, No. 6, pp. 2965-2989, 2008.
- [4] K.G. Van Der Zee, E. H. Van Brummelen and R. De Borst, Goal-oriented error estimation and adaptivity for free-boundary problems: the shape-linearization approach, *SIAM J. SCI. Comput.*, Vol. 32, No. 2, pp. 1093-1118, 2010.
- [5] J. Céa, Numerical methods of shape Optimal design, in "Optimization of Distributed Parameter Structures, vol II, E. J. Haug and J. Ca, eds., Sijhoff and Noordhoff, Alphen aan den Rijn, the Netherlands, 1981, pp. 1049-1087.
- [6] M.C. Delfour and J.P. Zolésio, Velocity method and Lagrangian formulation for the computation of the shape Hessian, *SIAM Control and Optimization*, Vol. 29, No. 6, pp. 1414-1442, 1991.
- [7] Roland Glowinski, Finite element methods for Navier-Stokes equations, *Annu. Rev. Fluid Mech.*, 1992, 24:167-204.
- [8] Demin Liu and Kaitai Li, Finite Element Analysis of the Stokes Equations with Damping, *Journal of Computational Mathematics* (in Chinese), 2010.

- [9] Demin Liu, *Mathematics Analysis and Numerical Methods for the Complex Viscous Flow and the Non-Newtonian Magnetohydrodynamic*, PhD thesis, Xi'an Jiaotong University, Shaanxi Province, 2010
- [10] R. Temam, *Navier-Stokes equation: Theory and Numerical Analysis*, Third edition, North-Holland, Amsterdam, New York, Oxford, 2003.
- [11] Max D. Gunzburger, *Perspectives in Flow Control and Optimization*, SIAM, Philadelphia, USA, 2002.
- [12] Kaitai Li, Jian Su, Limin Gao. Optimal shape design for blade's surface of an impeller via the Navier-Stokes equations. *Commun Numer Meth Engng*, 22:657-676, 2006.
- [13] Guang Xi, Zhiheng Wang, Chunmei Zhang, Minjian Yuan. Aerodynamic Optimization Design of Vaned Diffusers for the 100 kW Micro Gas Turbine's Centrifugal Compressor. ASME, GT2008-50440, 2008.
- [14] A Jameson, L Martinelli, NA Pierce. Optimum aerodynamic design using the Navier-Stokes equations. *Theor Comp Fluid Dyn*, 10: 213-237, 1998.
- [15] JL Lions. *Optimal control of systems governed by partial differential equations*. Berlin Heidelberg: Springer-Verlag, 1971.
- [16] Huiyuan Fan, Guang Xi, Shangjing Wang. Multi-point optimal design for diffuser cascades of centrifugal compressors. *Proc Instn Mech Engrs*, 214:187-190, 2000.
- [17] A Oyama, MS Liou. Transonic axial-flow blade optimization: Evolutionary algorithms/ three-dimensional Navier-Stokes solver. *Journal of Propulsion and Power*. 20(4): 612-619, 2004.
- [18] Xiaofeng Wang, Guang Xi, Zhiheng Wang. Aerodynamic optimization design of centrifugal compressor's impeller with Kriging model. *Proceeding of the Institution of Mechanical Engineers Part A-Journal of Power and energy*, 220(A6):585-597, 2006
- [19] J Li, YN He. A stabilized finite element method based on two local Gauss integrations for the Stokes equations, *J. Comp. Appl. Math.* 2008, 214:58-65.
- [20] Y He, J Li. A stabilized finite element method based on local polynomial pressure projection for the stationary Navier-Stokes equations. *Applied Numerical Mathematics*. 2008; 58(10):1503-1514.
- [21] HB Zheng, YR Hou, F Shi. Song LN. A finite element variational multiscale method for incompressible flows based on two local Gauss integrations, *J. Comput. Phys.* 2009, 228:5961-5977.
- [22] B. Mohammadi, O. Pironneau, *Applied Shape optimization for fluids*, Clarendon Press, Oxford, 2001.
- [23] M.C. Delfour, J.-P. Zolésio. *Shapes and Geometries: Analysis, Differential Calculus, and Optimization*, *Advance in Design and Control*. SIAM, 2002.
- [24] Jian Li, Zhangxin Chen. A new local stabilized nonconforming finite element method for the Stokes equations. *Computing*, 82(2-3): 157-170 (2008)
- [25] Jian Li, Zhangxin Chen. A new stabilized finite volume method for the stationary Stokes equations. *Adv. Comput. Math.* 30(2): 141-152 (2009)
- [26] Zhiming Gao, Yichen Ma, Shape gradient of the dissipated energy functional in shape optimization for the viscous incompressible flow. *Applied Numerical Mathematics* 58(2008)1720-1741.
- [27] Wenjing Yan, Yaling He and Yichen Ma. Shape inverse problem for the two-dimensional unsteady Stokes flow. *Numerical Methods for Partial Differential Equations*. 2010, 26(3), 690-701.
- [28] Kaitai Li, Rong An. On the Rotating Navier-Stokes Equations with Mixed Boundary Conditions, *Acta Mathematica Sinica, English Series*. *Numerical Methods for Partial Differential Equations*. 2008, Vol.24, No.4, 577-598.
- [29] P.B. Bochev, C.R. Dohmann, M.D. Gunzburger, Stabilization of low-order mixed finite elements for the Stokes equations, *SIAM J. Numer. Anal.* 2006, 44:82-101.
- [30] Zhiming Gao, Yichen Ma, A new stabilized finite element method for shape optimization in the steady Navier-Stokes flow. *Applied Numerical Mathematics*. 60(2010)816-832.
- [31] Tongjun Sun, Liang Ge, and Wenbing Liu. Equivalent a posteriori error estimates for a constrained optimal control problem governed by parabolic equations. *International Journal of Numerical Analysis and Modeling*. 2013, 10(1):1-23.

Center for Computational Geosciences, School of Mathematics and Statistics, Xi'an Jiaotong University, Shaanxi, 710049, P.R. China

E-mail: jsu@mail.xjtu.edu.cn

1.Center for Computational Geosciences, School of Mathematics and Statistics, Xi'an Jiaotong University, Shaanxi, 710049, P.R. China. 2. Department of Chemical and Petroleum Engineering, University of Calgary, Calgary, Alberta, T2N 1N4, Canada

E-mail: zhachen@ucalgary.ca

School of Energy and Power Engineering, Xian Jiaotong University, Xian 710049, P.R. China

E-mail: wangzhiheng@mail.xjtu.edu.cn and xiguang@mail.xjtu.edu.cn